Number of thermodynamic states in the three-dimensional Edwards-Anderson spin glass

Wenlong Wang,[1] Jonathan Machta,[2,3,*] Humberto Munoz-Bauza,[1,4] and Helmut G. Katzgraber[1,3]

[1]*Department of Physics and Astronomy, Texas A&M University, College Station, Texas 77843-4242, USA*
[2]*Department of Physics, University of Massachusetts, Amherst, Massachusetts 01003, USA*
[3]*Santa Fe Institute, 1399 Hyde Park Road, Santa Fe, New Mexico 87501, USA*
[4]*Department of Physics and Astronomy, University of Southern California, Los Angeles, California 90089, USA*

The question of the number of thermodynamic states present in the low-temperature phase of the three-dimensional Edwards-Anderson Ising spin glass is addressed by studying spin- and link-overlap distributions using population annealing Monte Carlo simulations. We consider overlaps between systems with the same boundary condition, which are the usual quantities measured, and also overlaps between systems with different boundary conditions, both for the full systems and also within a smaller window within the system. Our results appear to be fully compatible with a single pair of pure states such as in the droplet-scaling picture. However, our results for whether or not domain walls induced by changing boundary conditions are space filling or not are also compatible with scenarios having many thermodynamic states, such as the chaotic-pairs picture and the replica-symmetry-breaking picture. The differing results for spin overlaps in the same and different boundary conditions suggest that finite-size effects are very large for the system sizes currently accessible in low-temperature simulations.

I. INTRODUCTION

The nature of the low-temperature phase of Ising spin glasses is a long-standing mystery and the subject of considerable controversy [1–21]. A central question is whether the low-temperature phase is composed of a single pair of pure thermodynamic states or the situation is more complicated and involves an infinite number of pure states [22]. For many years, efforts to characterize the low-temperature phase were hampered by confusion over the concept of the thermodynamic limit for systems, such as spin glasses, that may display chaotic size dependence. Chaotic size dependence means that correlation functions within a finite observation volume fail to settle down as the system size is taken to infinity. If chaotic size dependence occurs, the usual thermodynamic limit is not meaningful and must be replaced by the so-called *metastate* [23–25], which is a probability distribution over thermodynamic states that may be observed in the observation volumes as the system size changes. Newman and Stein showed that the properties of the metastate are severely constrained for finite-dimensional spin glasses. The metastate either may be trivial and contain a single thermodynamic state consisting of a pair of pure states related by a global spin flip or may have support on an uncountable infinity of thermodynamic states. The *droplet picture*, developed by McMillan [26], Bray and Moore [27], and Fisher and Huse [28–30], is an example of the simple scenario where the metastate consists of a single pair of pure states and the thermodynamic limit may be defined in the usual way. There are two plausible ways that a metastate with support on a continuum of thermodynamic states could occur: either the *chaotic pairs* [25,31] scenario, where in every finite volume only a single pair of pure states is manifest, or the *nonstandard replica-symmetry-breaking* (RSB) scenario [25,32,33], where the thermodynamic states in the support of the metastate each consist of a countable infinity of pure states.

The nonstandard RSB scenario is the finite-dimensional analog of Parisi's replica-symmetry-breaking solution [22,34,35] of the mean-field Sherrington-Kirkpatrick model [36], i.e., the Ising spin glass on the complete graph. The idea that behavior similar to Parisi's RSB solution of the Sherrington-Kirkpatrick model also applies to the three-dimensional Ising spin glass has a long history [22,34,35,37–40], the nonstandard RSB scenario being the only mathematically well defined realization of the mean-field RSB theory in finite dimensions.

One of the key differences between scenarios with many thermodynamic states and a single pair of pure states is whether domain walls induced by changing boundary conditions are space filling. If there is a single thermodynamic state composed of a pair of pure states related by a global spin flip, then the relative domain wall induced by changing from periodic to antiperiodic boundary conditions in a single direction is not space filling. Given an observation window within a much larger system, this domain wall deflects out of the observation window, and a single pure state will be seen in the observation volume as the larger volume is taken to infinity. On the other hand, if there is chaotic size dependence and many thermodynamic states, then a change in boundary conditions is likely to induce a completely different thermodynamic state, and the relative domain wall will be space filling.

Many numerical studies have attempted to discern which theoretical picture correctly describes short-range systems (see, for example, Refs. [1–21]), resulting in often contradictory conclusions. Most notably, studies of the average distribution of the spin overlap, the order parameter for spin glasses, find a finite weight near zero overlap [5,6,9,12], suggesting a large multiplicity of pure states. However, because finite-size corrections are expected to be severe for currently available system sizes in simulations, new methods that go beyond simple disorder averaging have been developed to distinguish the different competing pictures [18,21,41–43]. These analyses, in contrast, suggest a thermodynamic limit with only a single pair of pure states.

*machta@physics.umass.edu

To further investigate this problem, in this work we set out to
determine whether relative domain walls induced by changing
boundary conditions (i.e., overlaps between configurations
with different boundary conditions) are space filling, and if
not, we measure their fractal dimension directly. To this end,
we carry out large-scale Monte Carlo simulations to study
the spin- and link-overlap distributions [9] and measure these
overlaps both in a single boundary condition and between spin
configurations chosen from different boundary conditions.
These measurements are made for both the full volume of
the studied system and an observation window smaller than
the full volume. Similar ideas have also been employed in
previous work. For example, spin-overlap distributions in a
small window with the same boundary condition were known
to be similar to those in the full system, which has been taken as
support of RSB in Ref. [44]. But when spin-overlap functions
in a small window between different boundary conditions
are studied, this is no longer clear. The spin-overlap and
link-overlap functions between different boundary conditions
at zero temperature have also been used in determining whether
domain walls are space filling in Refs. [6,45]; however,
these two studies reach opposite conclusions. Here we revisit
this problem systematically at nonzero temperatures. Our
results for the spin overlap from differing boundary conditions
point toward scenarios having a single thermodynamic state
consisting of a pair of pure states (as is the case for the droplet-
scaling picture). However, our results for the domain wall
induced by changing boundary conditions are also compatible
with many pairs of pure states as is the case for the RSB
and chaotic pairs picture. We therefore conclude that either
accessible system sizes in simulations are still too small despite
novel analysis techniques or the nature of the spin-glass state
is more complex than expected.

This paper is organized as follows. We first discuss
the model, observables, and simulation methods in Sec. II,
followed by numerical results in Sec. III. Concluding remarks
are stated in Sec. IV.

II. MODEL, OBSERVABLES, AND METHODS

We study the three-dimensional Edwards-Anderson (EA)
Ising spin-glass model [46] defined by the Hamiltonian

$$H = -\sum_{\langle ij \rangle} J_{ij} S_i S_j, \tag{1}$$

where $S_i = \pm 1$ are Ising spins and the sum is over nearest
neighbors on a cubic lattice of linear size L. The random
couplings J_{ij} are chosen from a Gaussian distribution with
mean 0 and variance 1. A set of couplings $\mathcal{J} = \{J_{ij}\}$ defines
a disorder realization.

We study two primary observables, the spin overlap q and
the link overlap q_ℓ, defined, respectively, as

$$q = \frac{1}{\lambda^3} \sum_i S_i^{(1)} S_i^{(2)} \tag{2}$$

and

$$q_\ell = \frac{1}{dL^3} \sum_{\langle ij \rangle} S_i^{(1)} S_j^{(1)} S_i^{(2)} S_j^{(2)}, \tag{3}$$

TABLE I. Parameters of the simulations for linear system sizes L
and for both periodic (π) and antiperiodic ($\overline{\pi}$) boundary conditions.
R_0 is the population size, $T_0 = 1/\beta_0$ is the lowest temperature
simulated, N_T is the number of temperatures used in the annealing
schedule, and N_{sa} is the number of disorder realizations.

L	R_0	$1/\beta_0$	N_T	M
4	5×10^4	0.200	101	4891
6	2×10^5	0.200	101	5000
8	5×10^5	0.200	201	4844
10	10^6	0.200	301	4600
12	10^6	0.333	301	4137

where spin configurations (1) and (2) are chosen independently
from the Boltzmann distribution. The sum in Eq. (2) is over
either the full lattice with $L \times L \times L$ sites or a smaller
observation window of size $W \times W \times W$ with $W < L$, and
for these two cases, $\lambda = L$ and $\lambda = W$, respectively. The
link overlap is measured only for the full lattice, and
the sum in Eq. (3) is over nearest neighbors. $d = 3$ is
the space dimension. Two boundary conditions are studied:
(i) periodic boundary conditions, referred to as π, and (ii)
periodic boundary conditions in the y and z directions with
antiperiodic boundary conditions in the x direction, referred
to as $\overline{\pi}$. The two boundary conditions differ in whether
$S_{\vec{r}+\hat{x}L} = \pm S_{\vec{r}}$, with the plus sign for π and the minus sign
for $\overline{\pi}$. Averages over the Gibbs distribution are indicated
with angular brackets, and the boundary condition for the two
copies required in the definition of an overlap are specified by
subscripts. For example, $\langle q_\ell \rangle_{\pi,\overline{\pi}}$ is the link overlap between
configurations (1) and (2) in boundary conditions π and $\overline{\pi}$,
respectively. We refer to overlaps between the same boundary
condition, either (π,π) or $(\overline{\pi},\overline{\pi})$, as *diagonal* overlaps and
overlaps between different boundary conditions, $(\pi,\overline{\pi})$ or
$(\pi,\overline{\pi})$, as *off-diagonal* overlaps.

We use population annealing Monte Carlo (PAMC) [47–50]
to carry out the simulations. In PAMC, a large population
of R_0 replicas of the system, each with the same disorder
realization, is annealed in parallel from infinite temperature to
a low target temperature, $T_0 = 1/\beta_0$. The annealing schedule
consists of a sequence of N_T temperatures equally spaced in
inverse temperature β. In a temperature step from β to β' the
population is resampled; some members of the population are
eliminated, and some are reproduced. The mean number of
copies of replica i is proportional to the reweighting factor,
$\exp[-(\beta' - \beta)E_i]$. The constant of proportionality is chosen
so that the population size remains close to R_0. Following each
resampling step, the population at β' is acted on by $N_S = 10$
lattice sweeps of the Metropolis algorithm. We simulate N_{sa}
disorder realizations and measure overlaps at $T = T_0 = 0.2$
and $T = 0.42$. Both of these temperatures are deep in the
low-temperature spin-glass phase and should therefore not be
affected by critical fluctuations. Overlaps are then measured by
pairing independent replicas in the population. The simulation
parameters are listed in Table I. A small number of disorder
realizations that were not equilibrated using population size
listed in Table I were rerun with larger populations until
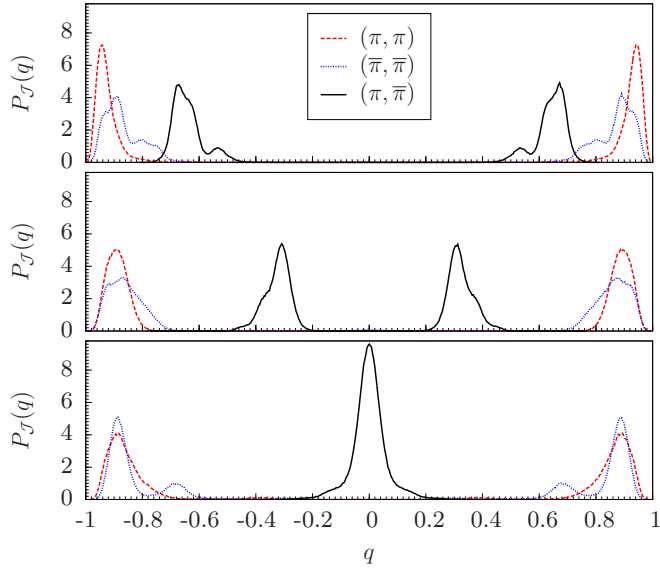equilibration was achieved.

FIG. 1. Spin-overlap distributions $P_\mathcal{J}(q)$ for three typical disorder realizations for $L = 8$ at $T = 0.42$. Each panel represents a different disorder realization, and within each panel, the overlap is shown for the boundary condition pairs (π, π) (red dashed line), $(\overline{\pi}, \overline{\pi})$ (blue dotted line), and $(\pi, \overline{\pi})$ (black solid line). The peaks in $P_\mathcal{J}(q)$ for the off-diagonal pair are shifted away from q_{EA} due to the relative domain wall between the periodic and antiperiodic boundary conditions.

III. RESULTS

We discuss the spin overlap in Sec. III A and the link overlap in Sec. III B. When possible, we carry out fits of the data assuming either space filling or non-space-filling domain walls and compare the quality of the fits.

A. Spin overlap

The spin-overlap distributions $P_\mathcal{J}(q)$ for three typical disorder realizations for the full system ($L = 8$ and $T = 0.42$) are shown in each of the three panels of Fig. 1. In each panel, the three curves represent the three boundary condition pairs (π, π), $(\overline{\pi}, \overline{\pi})$, and $(\pi, \overline{\pi})$. Observe that the two diagonal spin overlaps, (π, π) and $(\overline{\pi}, \overline{\pi})$, each have a peak(s) near the finite-size values of the Edwards-Anderson order parameter $\pm q_{EA}$. On the other hand, the off-diagonal overlap distributions have peaks that are shifted closer to the origin (i.e., $|q| < q_{EA}$) because the domain wall induced by changing boundary conditions reduces the probability of a large value of the spin overlap.

Figure 2 shows $P(q)$, the disorder-averaged spin-overlap distribution for sizes $L = 4, 6, 8, 10$, and 12 at $T = 0.42$ for the full lattice. The diagonal overlap distribution displays peaks at finite-size values of $\pm q_{EA}$, with q_{EA} decreasing with L, while for small q the distribution is nearly independent of L, consistent with past studies [5,9,12,18]. The off-diagonal overlap distribution, however, has *no* peaks close to $\pm q_{EA}$. Instead, the curves are nearly independent of L near $q = 0$ and seem to approach a relatively flat distribution bounded by $\pm q_{EA}$. It is instructive to compare this behavior with the ferromagnetic Ising model where the domain wall dimension is $d - 1$. Because a domain wall can be inserted anywhere in the system, $P(q)$ would have a flat distribution for $|q| \leqslant q_{EA}$.
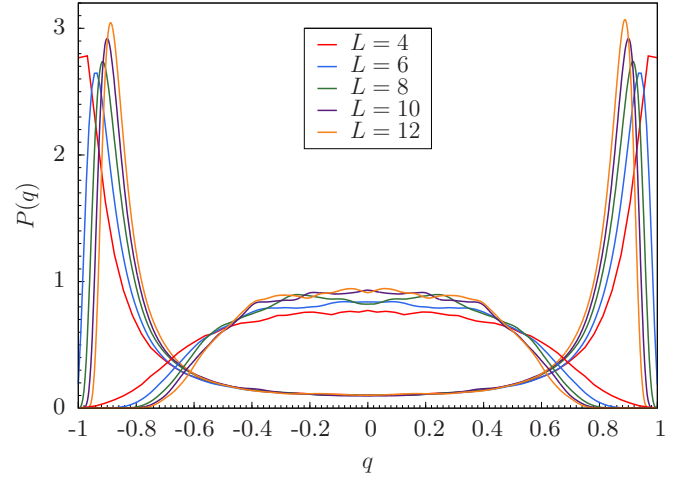

FIG. 2. Disorder-averaged spin-overlap distributions $P(q)$ for the full lattice for sizes $L = 4, 6, 8, 10$, and 12 at $T = 0.42$. The set of curves with peaks at the finite-size value of $\pm q_{EA}$ and bimodal features corresponds to the diagonal overlap distributions, while the set of curves with broad maxima at the center corresponds to the off-diagonal overlap distributions.

If a single thermodynamic state picture such as droplet scaling is correct for the EA model, the domain wall is expected to be fractal, and the off-diagonal $P(q)$ has a broad maximum at $q = 0$ with $P(q)$ decreasing toward $\pm q_{EA}$, just as is seen in Fig. 2. On the other hand, for many state scenarios such as RSB, changing boundary conditions almost always results in a completely different thermodynamic state so that the off-diagonal overlap distribution displays a δ function at the origin in the infinite-volume limit [51]. We see no evidence of a δ function at $q = 0$, and the behavior of the off-diagonal spin overlap therefore suggests a single pair of pure states.

To probe the behavior of the off-diagonal spin-overlap distribution more quantitatively, we also analyze four statistics of $P(q)$:

$P(0)$, the value of $P(q)$ at $q = 0$.
$\langle q^2 \rangle$, the second moment of $P(q)$.
$I(0.2) = \int_{|q| \leqslant 0.2} P(q) dq$.
f_q, the fraction of disorder realizations having a peak in the overlap distribution centered at $q = 0$.

If the relative domain wall is *space filling*, we expect that in the thermodynamic limit

$$P(0) \to \infty,$$
$$\langle q^2 \rangle \to 0,$$
$$I(0.2) \to 1,$$
$$f_q \to 1. \tag{4}$$

However, if the relative domain wall is a *fractal*

$$P(0) < \infty,$$
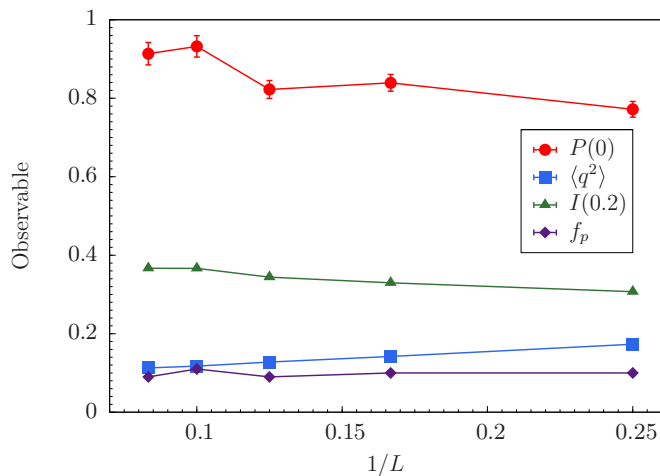$$\langle q^2 \rangle > 0,$$
$$I(0.2) < 1,$$
$$f_q < 1. \tag{5}$$

FIG. 3. Four statistics of the off-diagonal overlap distribution: $P(0)$, $\langle q^2 \rangle$, $I(0.2)$, and f_q (see text for details) vs inverse system size $1/L$. The expected thermodynamic behavior, i.e., $1/L \to 0$, is described in Eqs. (4) and (5).

Note that disorder averages are implied in the previous equations. The four statistics are shown in Fig. 3. One can see that indeed our data for the off-diagonal overlap distributions are compatible with a fractal relative domain wall and a single pair of pure states but are not compatible with multiple pure states and space-filling domain walls. The fact that the off-diagonal spin overlap suggests a single thermodynamic state scenario while the diagonal spin overlap suggests a thermodynamic scenario with multiple states implies very large finite-size corrections. This means that the average spin overlap cannot be used in currently accessible simulation system sizes to distinguish between these fundamentally different scenarios.

We next turn to the behavior of the spin overlap in an observation window of size W within a system of size $L \geqslant W$. Figure 4 shows spin-overlap distributions measured

in a window of size $W = 4$ within a system of size L with $L = 4, 6, 8, 10$, and 12 at $T = 0.42$. The curves with peaks at $\pm q_{EA}$ are the diagonal overlaps. These curves are only slightly dependent on the size of the full system, as first noted in Ref. [44]. On the other hand, the off-diagonal spin overlaps do evolve significantly with the size of the full system. It is notable that as L increases, peaks emerge at the finite-size value of the Edwards-Anderson order parameter. This phenomenon was observed qualitatively for ground states in three dimensions in Ref. [45] and suggests that the domain wall induced by switching boundary conditions might not be space filling and appears to deflect out of the window. If, as L becomes large, the off-diagonal and diagonal spin overlap become equal, this equality would be strong evidence in favor of the droplet-scaling picture. However, much larger system sizes would be needed to see such behavior.

To examine the behavior of the window overlap more quantitatively, we compare integrals of the diagonal and off-diagonal spin-overlap peaks in the region near $\pm q_{EA}$. We define Γ_s as the difference of the disorder-averaged diagonal and off-diagonal overlap distributions measured in the observation window and integrated over a set $\mathcal{A}$,

$$\Gamma_s = \frac{1}{2} \int_{\mathcal{A}} dq [P(q)_{\pi,\pi} + P(q)_{\bar{\pi},\bar{\pi}} - P(q)_{\pi,\bar{\pi}} - P(q)_{\bar{\pi},\pi}]. \tag{6}$$

We set $\mathcal{A} = [-1, -q_0) \cup (-q_0, 1]$, where q_0 is chosen to include the $\pm q_{EA}$ peaks. A similar quantity was studied for ground states in Ref. [45]. If there is indeed a single thermodynamic state and the domain wall deflects out of the window, then Γ_s should approach zero as $L \to \infty$. Furthermore, if the domain wall is a fractal with fractal dimension d_s, then we expect from box counting that

$$\Gamma_s \sim (L/W)^{d_s - d} \to 0 \quad \text{for} \quad L \to \infty, \tag{7}$$

where W is the window size, d_s is the fractal dimension of the domain wall, and $d = 3$ is the spatial dimension. A natural cutoff for measuring Γ_s is to set $q_0 = q_c$, where q_c is the crossing point of the off-diagonal spin overlap seen in Fig. 4.
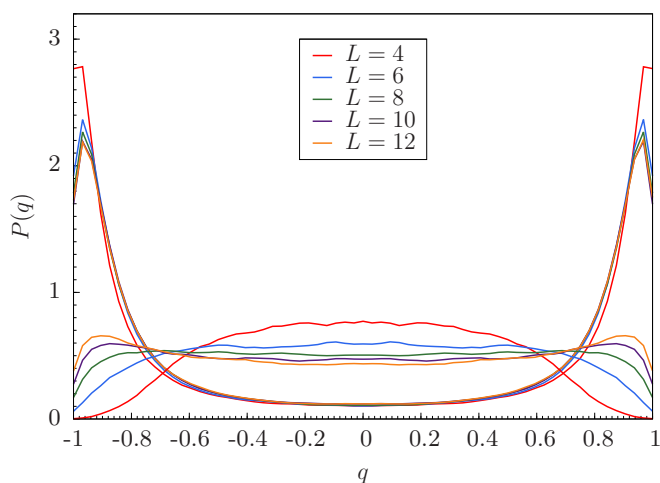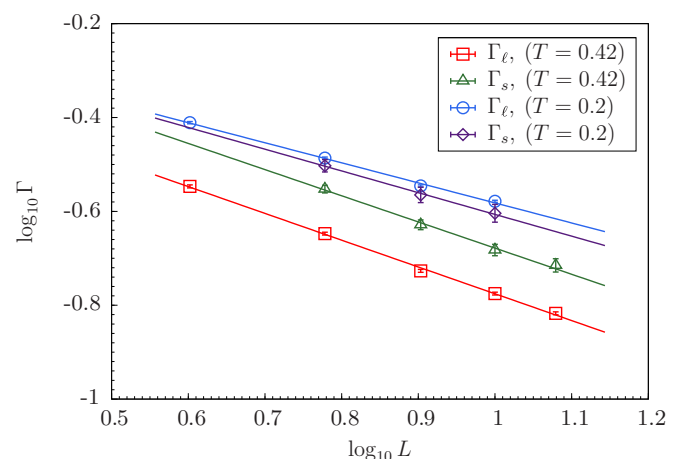

FIG. 4. Disorder-averaged spin-overlap distributions $P(q)$ in a $W = 4$ observation window within a system of size $L = 4, 6, 8, 10$, and 12 at $T = 0.42$. The sets of curves that display large peaks near $\pm q_{EA}$ are the diagonal overlaps. The off-diagonal overlap curves have much lower weight near $\pm q_{EA}$, but that weight increases slowly with the system size L.

FIG. 5. Scaling of Γ_s (within a window) and Γ_ℓ (defined below, for the full systems) as a function of system size L for $T = 0.20$ and $T = 0.42$ together with power-law fits (straight lines).
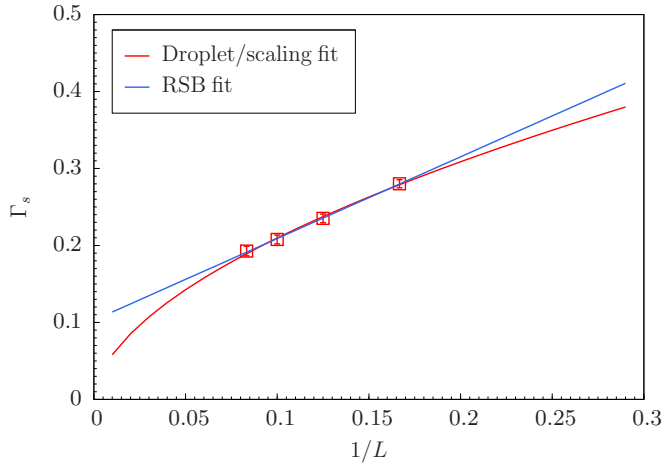
FIG. 6. Comparison of the fits of Γ_s assuming droplet scaling (red curved line, power law) or a RSB (blue straight line, constant and finite-size corrections) at $T = 0.42$. Both functional forms fit the data comparably well; that is, Γ_s does not distinguish the two pictures at these length scales. See text for details of fits.

For the $W = 4$ window, $q_c \approx 0.67$ for $T = 0.42$ and $q_c \approx 0.69$ for $T = 0.2$. Note, however, that our results are insensitive to the choice of q_0.

The scaling of Γ_s as a function of L is shown in Fig. 5. A fit of the form $\Gamma_s = a(L/W)^{d_s-d}$ yields $d_s = 2.44(3)$ and $a = 0.350(6)$ for $T = 0.42$ and $d_s = 2.54(3)$ and $a = 0.378(6)$ for $T = 0.2$, with quality of fit [52] $Q = 0.74$ and 0.80, respectively. Estimates of d_s are in reasonable agreement with previous results (e.g., Ref. [9]) before extrapolating the aforementioned values to zero temperature. This behavior suggests that the relative domain wall might be deflecting out of the observation window as L becomes much larger than W. If the trend continues, it would suggest a fractal domain wall and a single pair of pure states. However, a fit with the assumption of space-filling domain walls, i.e., $d_s = d$, of the form

$$\Gamma_s = a + b/(L/W) \rightarrow a \quad \text{for} \quad L \rightarrow \infty, \quad (8)$$

with $a = 0.103(3)$ and $b = 0.265(5)$, is of similar quality with $Q = 0.95$. The results of both fits at $T = 0.42$ are shown in Fig. 6. Therefore, the finite-size scaling of Γ_s is not able to distinguish between space-filling and non-space-filling domain walls at these length scales.

B. Link overlap

The average link overlap for diagonal and off-diagonal pairs of boundary conditions for the full system are shown in Fig. 7. In agreement with many previous studies, e.g., Ref. [9], the average diagonal link overlap is nearly independent of system size. On the other hand, the average off-diagonal link overlap is an increasing function of system size. If there is a single thermodynamic state and the relative domain wall induced by the change of boundary conditions is not space filling, then the diagonal and off-diagonal link-overlap distribution should become identical in the large-volume limit. To test this hypothesis, we consider the difference between diagonal and
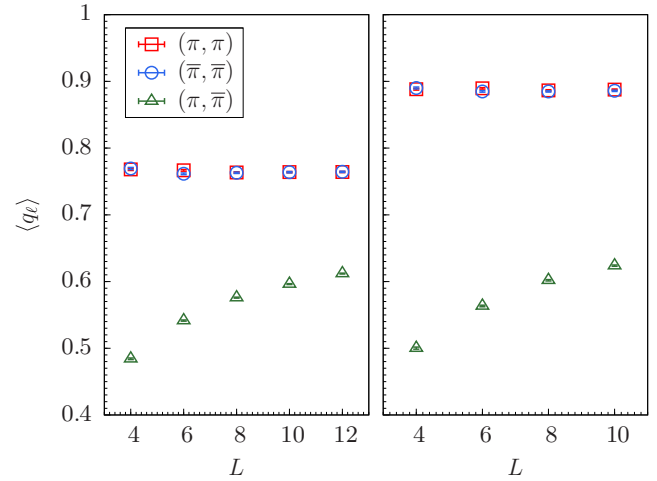
off-diagonal link overlaps,

$$\Gamma_\ell = [\![\langle q_\ell \rangle_{\pi,\pi} + \langle q_\ell \rangle_{\overline{\pi},\overline{\pi}} - \langle q_\ell \rangle_{\pi,\overline{\pi}} - \langle q_\ell \rangle_{\overline{\pi},\pi}]\!]/2, \quad (9)$$

where the double brackets indicate a disorder average. The difference between the diagonal and off-diagonal link overlaps is the average volume occupied by the relative domain wall induced by changing boundary conditions. Thus, if this domain wall has fractal dimension d_s and we compute Γ_ℓ in a system of size L, we again expect by box counting

$$\Gamma_\ell \sim L^{d_s-d}. \quad (10)$$

Figure 5 shows a log-log plot of Γ_ℓ as a function of L, and from a power-law fit, we estimate $d_s = 2.43(1)$ at $T = 0.42$ and $d_s = 2.57(2)$ at $T = 0.2$ with a quality of fit of $Q = 0.098$ and 0.017, respectively. These values (including the temperature
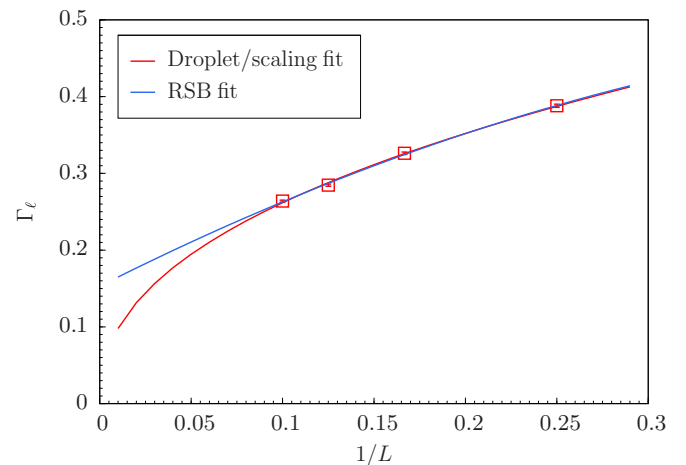

FIG. 7. Average of the link overlap $\langle q_\ell \rangle$ as a function of system size L for the three pairs of boundary conditions and temperatures $T = 0.42$ (left panel) and $T = 0.2$ (right panel). Note that as L increases, the off-diagonal link overlap increases toward the diagonal link overlap.

FIG. 8. Comparison of the fits of Γ_ℓ assuming droplet scaling (red lighter curve, power law) or a RSB (blue darker curve, constant and finite-size corrections) at $T = 0.2$. Both functional forms fit the data comparably well; that is, Γ_ℓ does not distinguish the two pictures at these length scales. See text for details of fits.

dependence) are in agreement with the results of Ref. [53]. Furthermore, the results at the lower temperature are in reasonable agreement with the zero-temperature estimates of Refs. [5,9].

However, fits with $\Gamma_\ell \to a > 0$, implying space-filling domain walls (i.e., $d_s = d$) and multiple thermodynamic states, are similarly satisfactory. For $T = 0.2$, a fit of the form $\Gamma_\ell = a + b/L + c/L^2$ yields $a = 0.15(2)$, $b = 1.2(3)$, and $c = 1.0(7)$ with $Q = 0.03$. The uncertainty in c is very large because of the shape of the error ellipse of the three-parameter fit, but it should be noted that a two-parameter fit with c set to zero is of much lower quality, although it has a similar value of a. This RSB fit is shown in Fig. 8 along with the two-parameter power-law fit $\Gamma_\ell = aL^{(d_s-3)}$, with $a = 0.7(2)$ and $d_s = 2.57(2)$, with $Q = 0.017$. Neither fit is high quality, and Γ_ℓ cannot distinguish the two scenarios at these length scales.

IV. SUMMARY AND FUTURE CHALLENGES

We have investigated the spin and link overlaps between the same and different boundary conditions for the full system as well as in a smaller observation window in the three-dimensional Edwards-Anderson Ising spin glass. We have found that the *off-diagonal* spin-overlap function for the full system is relatively flat and nearly independent of system size, in agreement with a single thermodynamic state consisting of a pair of pure states. This metric not used to date represents another way to differentiate different theoretical scenarios.

On the other hand, as has been noted in previous studies, the *diagonal* spin-overlap function is nonzero and nearly independent of systems size near $q = 0$, which supports scenarios with many thermodynamic states. The two sets of results together imply that for system sizes currently accessible to low-temperature simulations, the average spin overlap is incapable of distinguishing the two scenarios for the three-dimensional Edwards-Anderson model. A detailed analysis of the link overlap and the spin overlap in a window is consistent with fractal domain walls that have a fractal dimension near $d_s \approx 2.5$. However, we cannot rule out space-filling domain walls.

While the use of $1/L$ finite-size corrections is reasonable for the studied system sizes and hence we cannot rule out space-filling domain walls, we believe it is an important future challenge to find a theoretical basis for the used scaling form. In contrast, the ground-state energy per spin e has corrections that scale as $e = a + b/L^x$, where $x = d - \theta \approx 2.76$ in three dimensions [54]. This exponent is much larger, and using such a large exponent, the space-filling fits for our data are no longer satisfactory. While it is possible that different quantities may show different finite-size corrections at the zero-temperature fixed point, it is still important to find a theoretical basis to explain why the $1/L$ corrections are needed when studying the scaling of the link overlap yet not for the ground-state energy per spin.

Substantially larger system sizes would be required to clearly determine whether domain walls induced by changing boundary conditions are space filling or not using average spin overlaps in windows or link overlaps. Since the first large-scale simulations in 2001, approximately 16 years have passed. Betting on Moore's law [55], we expected to be able to revisit this problem and bring more clarity to the different theoretical descriptions of the spin-glass state. However, our results clearly show that more effort needs to be put into the development of better algorithms, as well as new statistics to tackle these problems.

[1] M. Mézard, G. Parisi, N. Sourlas, G. Toulouse, and M. Virasoro, Nature of the Spin-Glass Phase, Phys. Rev. Lett. **52**, 1156 (1984).

[2] M. A. Moore, H. Bokil, and B. Drossel, Evidence for the Droplet Picture of Spin Glasses, Phys. Rev. Lett. **81**, 4252 (1998).

[3] B. Drossel, H. Bokil, M. A. Moore, and A. J. Bray, The link overlap and finite size effects for the 3D Ising spin glass, Euro. Phys. J. **13**, 369 (2000).

[4] F. Krzakala and O. C. Martin, Spin and Link Overlaps in Three-Dimensional Spin Glasses, Phys. Rev. Lett. **85**, 3013 (2000).

[5] M. Palassini and A. P. Young, Nature of the Spin Glass State, Phys. Rev. Lett. **85**, 3017 (2000).

[6] E. Marinari and G. Parisi, On the effects of changing the boundary conditions on the ground state of Ising spin glasses, Phys. Rev. B **62**, 11677 (2000).

[7] E. Marinari, G. Parisi, F. Ricci-Tersenghi, J. J. Riuz-Lorenzo, and F. Zuliani, Replica symmetry breaking in short range spin glasses: A review of the theoretical foundations and of the numerical evidence, J. Stat. Phys. **98**, 973 (2000).

[8] E. Marinari, G. Parisi, F. Ricci-Tersenghi, and J. J. Ruiz-Lorenzo, Off-equilibrium dynamics at very low temperatures in three-dimensional spin glasses, J. Phys. A **33**, 2373 (2000).

[9] H. G. Katzgraber, M. Palassini, and A. P. Young, Monte Carlo simulations of spin glasses at low temperatures, Phys. Rev. B **63**, 184422 (2001).

[10] A. A. Middleton, Energetics and geometry of excitations in random systems, Phys. Rev. B **63**, 060202(R) (2001).

[11] N. Hatano and J. E. Gubernatis, Evidence for the droplet picture in the three-dimensional $\pm J$ spin glass, Phys. Rev. B **66**, 054437 (2002).

[12] H. G. Katzgraber and A. P. Young, Monte Carlo simulations of spin-glasses at low temperatures: Effects of free boundary conditions, Phys. Rev. B **65**, 214402 (2002).

[13] H. G. Katzgraber and A. P. Young, Monte Carlo studies of the one-dimensional Ising spin glass with power-law interactions, Phys. Rev. B **67**, 134410 (2003).

[14] H. G. Katzgraber and A. P. Young, Geometry of large-scale low-energy excitations in the one-dimensional Ising spin glass with power-law interactions, Phys. Rev. B **68**, 224408 (2003).

[15] G. Hed and E. Domany, Nontrivial link overlap distribution in three-dimensional Ising spin glasses, Phys. Rev. B **76**, 132408 (2007).

[16] L. Leuzzi, G. Parisi, F. Ricci-Tersenghi, and J. J. Ruiz-Lorenzo, Diluted One-Dimensional Spin Glasses with Power Law Decaying Interactions, Phys. Rev. Lett. **101**, 107203 (2008).

[17] R. A. Baños, A. Cruz, L. A. Fernandez, J. M. Gil-Narvion, A. Gordillo-Guerrero, M. Guidetti, A. Maiorano, F. Mantovani, E. Marinari, V. Martin-Mayor *et al.*, Nature of the spin-glass phase at experimental length scales, J. Stat. Mech. (2010) P06026.

[18] B. Yucesoy, H. G. Katzgraber, and J. Machta, Evidence of Non-Mean-Field-Like Low-Temperature Behavior in the Edwards-Anderson Spin-Glass Model, Phys. Rev. Lett. **109**, 177204 (2012).

[19] A. Billoire, L. A. Fernandez, A. Maiorano, E. Marinari, V. Martin-Mayor, G. Parisi, F. Ricci-Tersenghi, J. J. Ruiz-Lorenzo, and D. Yllanes, Comment on "Evidence of Non-Mean-Field-Like Low-Temperature Behavior in the Edwards-Anderson Spin-Glass Model," Phys. Rev. Lett. **110**, 219701 (2013).

[20] B. Yucesoy, H. G. Katzgraber, and J. Machta, Yucesoy, Katzgraber, and Machta Reply, Phys. Rev. Lett. **110**, 219702 (2013).

[21] W. Wang, J. Machta, and H. G. Katzgraber, Evidence against a mean-field description of short-range spin glasses revealed through thermal boundary conditions, Phys. Rev. B **90**, 184412 (2014).

[22] G. Parisi, Infinite Number of Order Parameters for Spin-Glasses, Phys. Rev. Lett. **43**, 1754 (1979).

[23] M. Aizenman and J. Wehr, Rounding effects of quenched randomness on first-order phase transitions, Commun. Math. Phys. **130**, 489 (1990).

[24] C. M. Newman and D. L. Stein, Spatial Inhomogeneity and Thermodynamic Chaos, Phys. Rev. Lett. **76**, 4821 (1996).

[25] C. M. Newman and D. L. Stein, Metastate approach to thermodynamic chaos, Phys. Rev. E **55**, 5194 (1997).

[26] W. L. McMillan, Domain-wall renormalization-group study of the two-dimensional random Ising model, Phys. Rev. B **29**, 4026 (1984).

[27] A. J. Bray and M. A. Moore, Scaling theory of the ordered phase of spin glasses, in *Heidelberg Colloquium on Glassy Dynamics and Optimization*, edited by L. Van Hemmen and I. Morgenstern (Springer, New York, 1986), p. 121.

[28] D. S. Fisher and D. A. Huse, Ordered Phase of Short-Range Ising Spin-Glasses, Phys. Rev. Lett. **56**, 1601 (1986).

[29] D. S. Fisher and D. A. Huse, Absence of many states in realistic spin glasses, J. Phys. A **20**, L1005 (1987).

[30] D. S. Fisher and D. A. Huse, Equilibrium behavior of the spin-glass ordered phase, Phys. Rev. B **38**, 386 (1988).

[31] C. M. Newman and D. L. Stein, Multiple states and thermodynamic limits in short-ranged Ising spin-glass models, Phys. Rev. B **46**, 973 (1992).

[32] N. Read, Short-range Ising spin glasses: The metastate interpretation of replica symmetry breaking, Phys. Rev. E **90**, 032142 (2014).

[33] A. Billoire, L. A. Fernandez, A. Maiorano, E. Marinari, V. Martin-Mayor, J. Moreno-Gordo, G. Parisi, F. Ricci-Tersenghi, and J. J. Ruiz-Lorenzo, Numerical Construction of the Aizenman-Wehr Metastate, Phys. Rev. Lett. **119**, 037203 (2017).

[34] G. Parisi, The order parameter for spin glasses: A function on the interval 0–1, J. Phys. A **13**, 1101 (1980).

[35] G. Parisi, Order Parameter for Spin-Glasses, Phys. Rev. Lett. **50**, 1946 (1983).

[36] D. Sherrington and S. Kirkpatrick, Solvable Model of a Spin Glass, Phys. Rev. Lett. **35**, 1792 (1975).

[37] R. Rammal, G. Toulouse, and M. A. Virasoro, Ultrametricity for physicists, Rev. Mod. Phys. **58**, 765 (1986).

[38] M. Mézard, G. Parisi, and M. A. Virasoro, *Spin Glass Theory and Beyond* (World Scientific, Singapore, 1987).

[39] *Spin Glasses and Random Fields*, edited by A. P. Young (World Scientific, Singapore, 1998).

[40] G. Parisi, Some considerations of finite dimensional spin glasses, J. Phys. A **41**, 324002 (2008).

[41] A. A. Middleton, Extracting thermodynamic behavior of spin glasses from the overlap function, Phys. Rev. B **87**, 220201 (2013).

[42] C. Monthus and T. Garel, Typical versus averaged overlap distribution in spin glasses: Evidence for droplet scaling theory, Phys. Rev. B **88**, 134204 (2013).

[43] M. Wittmann, B. Yucesoy, H. G. Katzgraber, J. Machta, and A. P. Young, Low-temperature behavior of the statistics of the overlap distribution in Ising spin-glass models, Phys. Rev. B **90**, 134419 (2014).

[44] E. Marinari, G. Parisi, F. Ricci-Tersenghi, and J. J. Ruiz-Lorenzo, Small window overlaps are effective probes of replica symmetry breaking in three-dimensional spin glasses, J. Phys. A **31**, L481 (1998).

[45] M. Palassini and A. P. Young, Triviality of the Ground State Structure in Ising Spin Glasses, Phys. Rev. Lett. **83**, 5126 (1999).

[46] S. F. Edwards and P. W. Anderson, Theory of spin glasses, J. Phys. F **5**, 965 (1975).

[47] K. Hukushima and Y. Iba, Population Annealing and its application to a spin glass, in *The Monte Carlo Method in the Physical Sciences: Celebrating the 50th Anniversary of the Metropolis Algorithm*, edited by J. E. Gubernatis, AIP Conf. Proc. No. 690 (AIP, Melville, NY, 2003), p. 200.

[48] E. Zhou and X. Chen, A new population-based simulated annealing algorithm, in *Proceedings of the 2010 Winter Simulation Conference (WSC)* (Springer, Baltimore, 2010), p. 1211.

[49] J. Machta, Population annealing with weighted averages: A Monte Carlo method for rough free-energy landscapes, Phys. Rev. E **82**, 026704 (2010).

[50] W. Wang, J. Machta, and H. G. Katzgraber, Population annealing: Theory and application in spin glasses, Phys. Rev. E **92**, 063307 (2015).

[51] T. Aspelmeier, W. Wang, M. A. Moore, and H. G. Katzgraber, Interface free-energy exponent in the one-dimensional Ising spin glass with long-range interactions in both the droplet and broken replica symmetry regions, Phys. Rev. E **94**, 022116 (2016).

[52] W. H. Press, S. A. Teukolsky, W. T. Vetterling, and B. P. Flannery, *Numerical Recipes in C* (Cambridge University Press, Cambridge, 1995).

[53] W. Wang, J. Machta, and H. G. Katzgraber, Chaos in spin glasses revealed through thermal boundary conditions, Phys. Rev. B **92**, 094410 (2015).

[54] S. Boettcher and S. Falkner, Finite-size corrections for ground states of Edwards-Anderson spin glasses, Eur. Phys. Lett. **98**, 47005 (2012).

[55] G. Moore, Cramming more components onto integrated circuits, Electron. Mag. **38**, 114 (1965).